

*Dedicated to Professor Alexandru T. Balaban
on the occasion of his 85th anniversary*

TWO Zn(II) DISTORTION ISOMERS IN A SINGLE CRYSTAL. SYNTHESIS, SUPRAMOLECULAR INTERACTIONS AND THERMAL ANALYSIS

Carmen PARASCHIV,^{a,*} Andrei CUCOS,^a Sergiu SHOVA^b and Marius ANDRUH^c

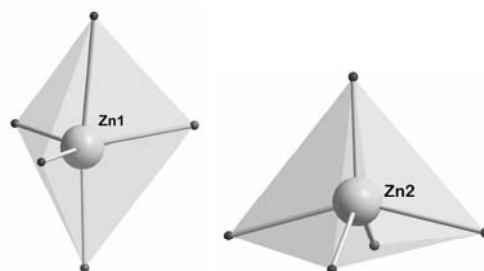
^aNational Institute for Research and Development in Electrical Engineering ICPE-CA,
Splaiul Unirii 313, 030138-Bucharest, Roumania

^b“Petru Poni” Institute of Macromolecular Chemistry of the Roumanian Academy, Aleea Grigore Ghica Voda 41-A,
RO-700487 Iași, Roumania

^cInorganic Chemistry Laboratory, Faculty of Chemistry, University of Bucharest, Str. Dumbrava Roșie 23,
020464-Bucharest, Roumania

Received August 6, 2015

A new mononuclear complex, $[\text{Zn}(\text{H}_3\text{tris})_2(1,3\text{-bdc})]$ **1** (H_3tris = tris(hydroxymethyl)aminomethane, $1,3\text{-H}_2\text{bdc}$ = 1,3-benzenedicarboxylic acid), was synthesized solvothermally and characterized by single crystal and powder X-ray diffraction, IR spectroscopy, and thermal analysis under synthetic air atmosphere using the coupled TG-FTIR method. The asymmetric unit contains two distortion isomers. Slight variations in the bond lengths and angles within the chromophores impose different geometries for the zinc atoms in the two isomers. The 3D supramolecular network, formed through plentiful H-bonds and weak molecular interactions, has been analyzed.



INTRODUCTION

The past decades have witnessed tremendous progress in crystal engineering.¹ One of the challenges is to improve our understanding of how the balance between strong/weak forces determines the assembly of the molecules in the crystal. Hydrogen bonding is undoubtedly the most efficient and widely used non-covalent tool for molecular self-assembly by reason of its strong directing capability, selectivity and reversible formation at room temperature.² The O–H...O hydrogen bonds formed by –COOH and –OH groups are among the strongest non-covalent interactions. Furthermore, the

O–H...O bond can be strengthened if the polarity of the acceptor is increased *via* deprotonation of the carboxylic group. These interactions are sufficiently strong to influence recognition and self-assembly of carboxylic acid/carboxylate anions in high dimensional superstructures.³

Nowadays hydro- or solvothermal synthesis is one of the most popular methods to obtain coordination networks despite the fact that the synthetic target is not always reached and chance and serendipity often affect the outcome of the reaction.⁴ The issue of mixtures of phases, and particularly amorphous components, is a problem faced by many researchers using this synthetic method.

* Corresponding authors: carmenparaschiv@yahoo.com

In a previous work we described a series of zinc(II) coordination polymers assembled in the presence of amino-alcohols and aromatic dicarboxylic acids.⁵ In the attempt to prepare the tris(hydroxymethyl)aminomethane – 1,3-benzenedicarboxylate system we obtained two compounds, depending on the zinc source. Firstly, when using $\text{Zn}(\text{NO}_3)_2$, the $[\text{Zn}(\text{H}_3\text{tris})(1,3\text{-bdc})(\text{CH}_3\text{OH})]$ coordination polymer is formed.⁵ The structure consists of $[\text{Zn}(\text{H}_3\text{tris})(\text{CH}_3\text{OH})]^{2+}$ nodes connected by bridging isophthalato ligands to afford a linear chain. The chains are further interconnected into a complex non-covalent 3D network through hydrogen bonds involving the coordinated and uncoordinated OH groups of the H_3tris ligand, the carboxylato oxygen atoms and the oxygen atoms from the methanol ligands. In the present paper we report the product of the reaction between ZnO , H_3tris , and isophthalate anion, namely the mononuclear complex $[\text{Zn}(\text{H}_3\text{tris})_2(1,3\text{-bdc})]$ **1**. This system is a rare case of distortion isomers that cocrystallize in the same compound, very few examples being described in the literature so far.⁶

RESULTS AND DISCUSSION

Compound **1** crystallizes in the monoclinic system, space group P_12_11 , with cell parameters and structure refinement details given in Table 1. The asymmetric unit contains two crystallographically independent neutral mononuclear $[\text{Zn}(\text{H}_3\text{tris})_2(1,3\text{-bdc})]$ entities, which

are labeled as molecule A and B, respectively (Fig. 1). The H_3tris molecules are not deprotonated and coordinate as bidentate chelating ligands toward the zinc(II) ions through the nitrogen and one oxygen atom, while the other two OH groups remain uncoordinated. Both zinc atoms are five-coordinated by two nitrogen and two oxygen atoms from the H_3tris bidentate ligands and an oxygen atom provided by a monodentate isophthalate anion, but their coordination geometries are different. In the type-A mononuclear unit, the Zn1 ion displays a distorted trigonal bipyramidal environment, with the trigonal distortion parameter τ^7 of 0.76 (Fig. 2, left). The equatorial plane is occupied by one oxygen atom from a H_3tris molecule, the nitrogen atom from the other H_3tris ligand and one oxygen from the isophthalate ligand [$\text{Zn1-O1} = 2.021(4)$; $\text{Zn1-N2} = 2.033(3)$; $\text{Zn1-O7} = 1.945(5)$ Å], while the axial positions are filled by one amino nitrogen and one oxygen atom from the two amino-alcohol ligands [$\text{Zn1-N1} = 2.120(3)$; $\text{Zn1-O6} = 2.361(3)$ Å]. In the type-B entity, the Zn2 ion shows a distorted square pyramidal geometry, with the value of the parameter τ equal to 0.4 (Fig. 2, right). The basal plane is defined by two oxygen and two nitrogen atoms from the H_3tris chelating molecules [$\text{Zn2-O11} = 2.150(4)$; $\text{Zn2-O14} = 2.052(4)$; $\text{Zn2-N3} = 2.145(4)$; $\text{Zn2-N4} = 2.061(3)$ Å], while the fifth coordination site is occupied by the oxygen atom from the isophthalate ligand [$\text{Zn2-O17} = 1.942(5)$ Å].

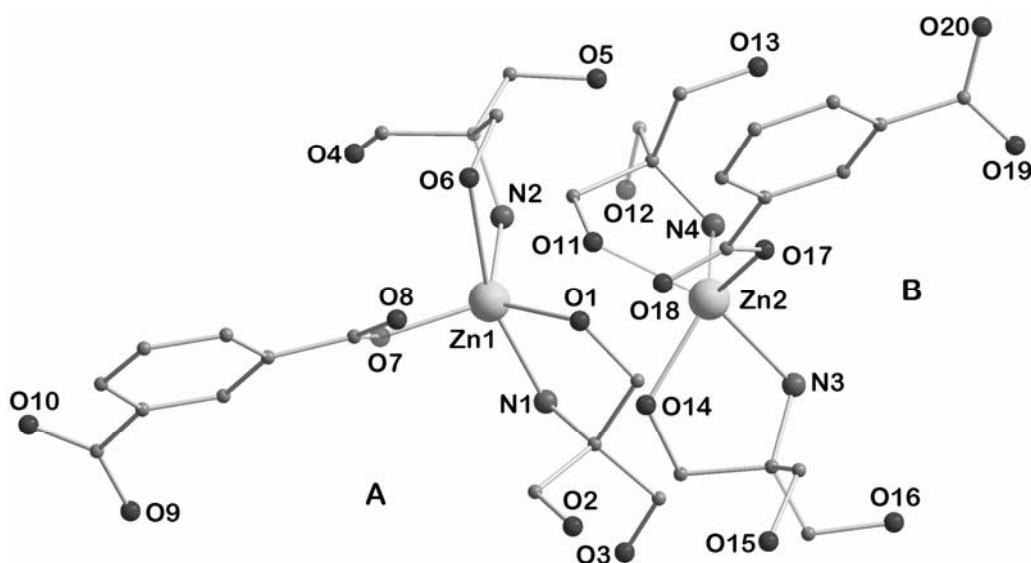


Fig. 1 – The asymmetric unit in **1** with the atom labeling scheme. Hydrogen atoms have been omitted.

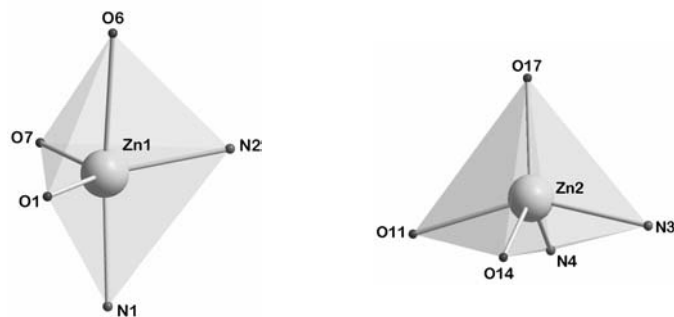
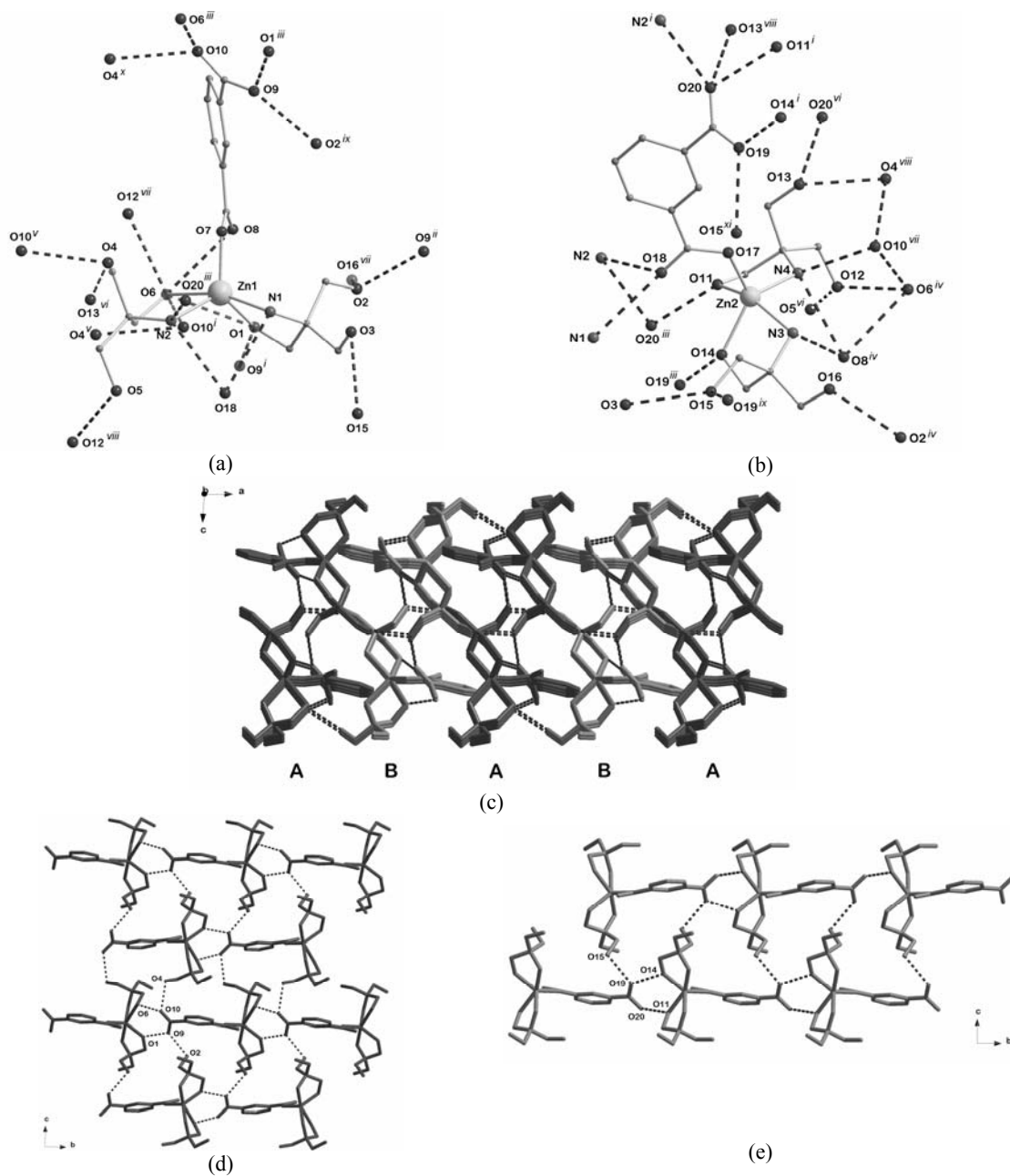
Fig. 2 – Coordination polyhedra of the Zn1 and Zn2 atoms in **1**.

Fig. 3 – Fragments of the crystal packing of **1**: (a)–(b) the hydrogen bonds formed by the two distortion isomers; (c) the 3D supramolecular hydrogen-bonded network; (d) supramolecular layers constructed from hydrogen-bonded type-A molecules; (e) a supramolecular double chain formed by the type-B mononuclear entities. Symmetry codes: ⁱ = $x, 1+y, z$; ⁱⁱ = $-x, 1/2+y, 1-z$; ⁱⁱⁱ = $x, -1+y, z$; ^{iv} = $1+x, y, z$; ^v = $-x, 1/2+y, -z$; ^{vi} = $1-x, -1/2+y, -z$; ^{vii} = $1+x, 1+y, z$; ^{viii} = $1-x, 1/2+y, -z$; ^{ix} = $1-x, -1/2+y, 1-z$; ^x = $-x, -1/2+y, -z$; ^{xi} = $1-x, 1/2+y, 1-z$.

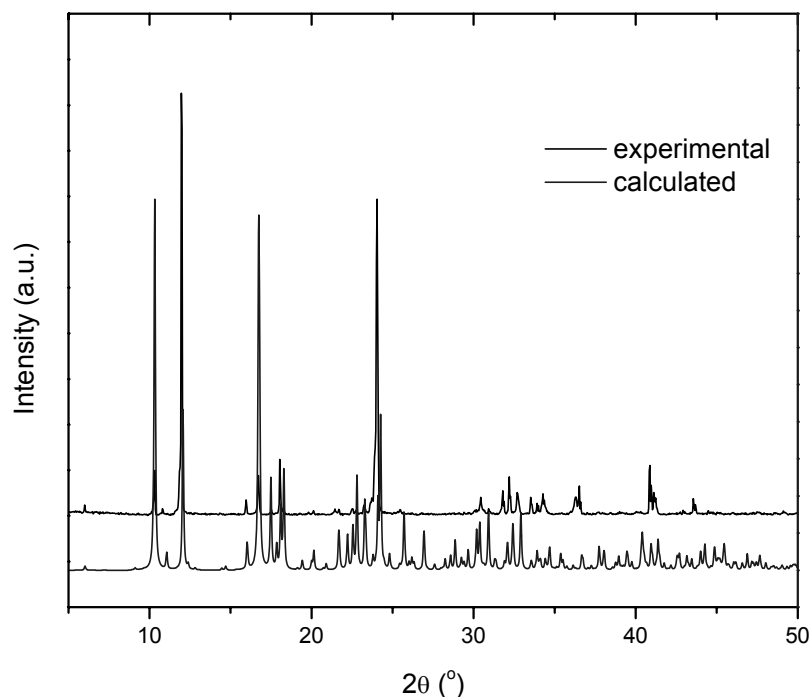


Fig. 4 – Powder X-ray diffraction patterns of **1**. Above: experimental data; below: calculated from single crystal diffraction data.

The neutral $[\text{Zn}(\text{H}_3\text{tris})_2(1,3\text{-bdc})]$ units are linked in the *ABAB* sequence (Fig. 3c) through hydrogen-bonds involving the isophthalate oxygen atoms, the amino nitrogen atoms and the coordinated and uncoordinated OH groups from the amino-alcohol, leading to a complex three-dimensional supramolecular network. Details of the H-bonding schemes for the two distortion isomers are given in Fig. 3a-b. The type-A mononuclear units are interconnected through H-bonds in supramolecular layers which are parallel to the *bc* plane (Fig. 3d), while the type-B entities form supramolecular double chains growing along the crystallographic *b* axis (Fig. 3e). The distances between the donor and the acceptor vary between 2.572(6) and 3.082(4) Å for the O-H \cdots O interactions and are in the 2.801(6) – 3.021(6) Å range for the N-H \cdots O contacts. The parameters associated to the intra- and intermolecular hydrogen bond interactions are presented in Table 3.

Comparison of the experimental X-ray powder pattern with the one calculated from single-crystal data revealed a pure phase of compound **1** (Fig. 4).

Thermal stability studies

TG data (Fig. 5) show that compound **1** is stable up to about 210 °C. Above this temperature, thermal decomposition sets in, characterized by

four peaks in DTG at 230, 264, 406 °C (the main one) and 487 °C, and several peaks in DTA (219 °C – endothermic, 357, 397, 413 and 487 °C – exothermic peaks, the latter being the strongest). The Gram Schmidt curve shows two strong peaks at 411 °C and 491 °C. The decomposition ends at about 500 °C, when the expected amount of ZnO is formed (calculated: 17.3%, found: 16.7%).

The analysis of the FTIR spectra of the evolved gases (Fig. 5) revealed a strong release of water vapors starting from 220 °C. At above 280 °C the intense bands of CO₂ appear (originating, at this stage, from the oxidation of the aliphatic side chains of H₃tris ligands), together with the characteristic sharp bands of ammonia. This intense generation of ammonia is readily explained by the deamination of H₃tris ligands that possess a primary –NH₂ group. Nitrogen from the amino-alcohol can also be oxidized and released as N₂O (that starts to evolve at above 300 °C) and NO, both with maximum evolutions at ~470 °C, corresponding to the last decomposition process. Isophthalate ligands undergo total decarboxylation, as confirmed by the observation of a very strong band assigned to benzene at about 420 °C. No traces of benzoic acid, indicative of partial decarboxylation, were detected. The bands of methane and CO are also observed in the FTIR spectra.

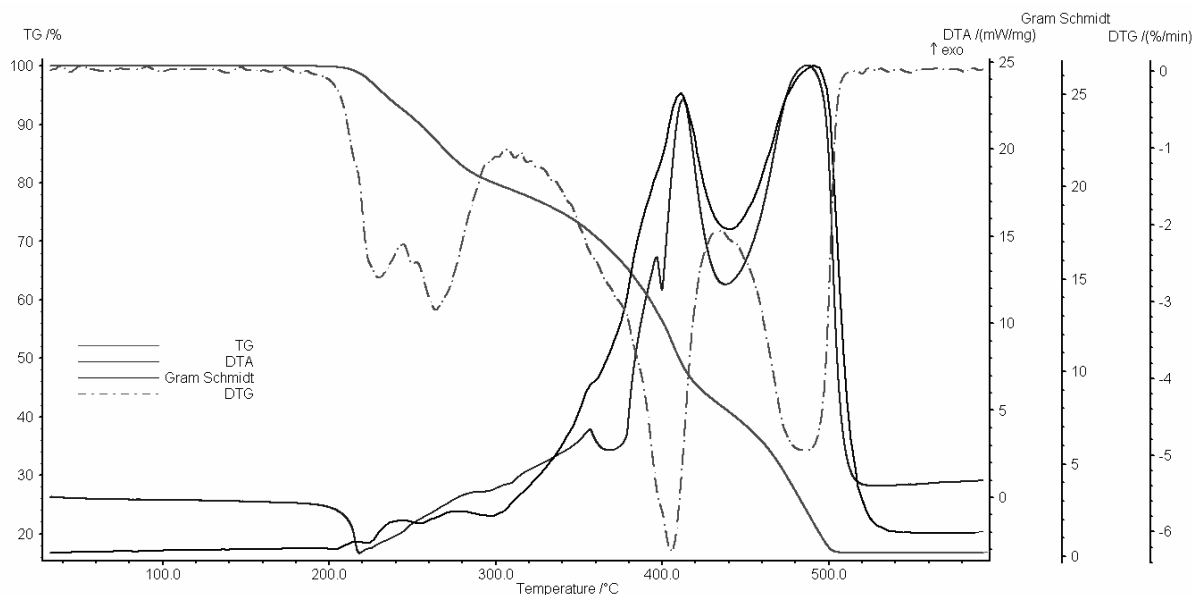


Fig. 4 – TG, DTG, DTA and Gram Schmidt curves for compound 1.

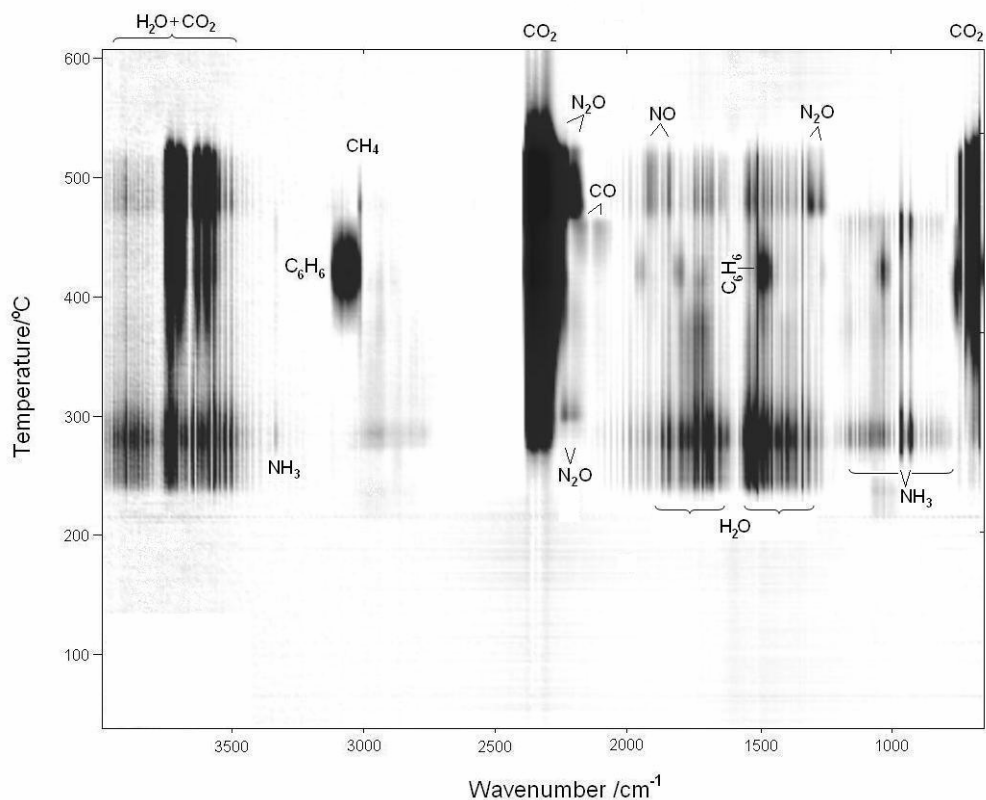


Fig. 5 – 2D plot of FTIR spectra of gases evolved from the decomposition of 1.

The system described in this paper is a rare case of two distortion isomers in the same crystal lattice. The two isomers differ by the stereochemistries of the Zn1 and Zn2 atoms. At supramolecular level, this compound illustrates the versatility of hydrogen bonding interaction for the non-covalent solid state assembly of mononuclear

complexes into high dimensional supramolecular architectures. Along with the system described in our earlier report,⁵ it also demonstrates the unpredictability of the solvothermal synthesis, since slight variations of the synthetic conditions led to the formation of two different compounds.

Table 1

Crystallographic data, details of data collection and structure refinement parameters for **1**

Empirical formula	C ₃₂ H ₅₂ Zn ₂ N ₄ O ₂₀
M (g mol ⁻¹)	943.52
Temperature (K)	160.0(1)
Wavelength (Å)	0.71073
Crystal system	monoclinic
Space group	<i>P</i> ₁ 2 ₁ 1
<i>a</i> [Å]	12.2665(3)
<i>b</i> [Å]	10.5550(3)
<i>c</i> [Å]	14.6905(3)
β [°]	93.520(2)
<i>V</i> [Å ³]	1898.44(8)
<i>Z</i>	4
ρ (calcd) [Mgm ⁻³]	1.651
μ [mm ⁻¹]	1.354
<i>F</i> (000)	984
Gof (for <i>F</i> 2)	1.043
Final <i>R</i> , <i>wR</i> [<i>I</i> > 2 σ (<i>I</i>)]	0.0362, 0.0807
$\Delta\rho_{\max}$ and $\Delta\rho_{\min}$ [e Å ⁻³]	0.492 and -0.473

Table 2

Selected bond distances (Å) and angles (°) for compound **1**

Zn1–O1	2.021(4)	O1–Zn1–O6	86.12(14)
Zn1–O6	2.361(3)	O1–Zn1–N1	80.38(16)
Zn1–O7	1.945(5)	O1–Zn1–N2	120.20(19)
Zn1–N1	2.120(3)	O7–Zn1–O1	120.96(15)
Zn1–N2	2.033(3)	O7–Zn1–O6	92.02(15)
Zn2–O11	2.150(4)	O7–Zn1–N1	105.01(18)
Zn2–O14	2.052(4)	O7–Zn1–N2	116.57(18)
Zn2–O17	1.942(5)	N1–Zn1–O6	162.1(2)
Zn2–N3	2.145(4)	N2–Zn1–O6	76.75(13)
Zn2–N4	2.061(3)	N2–Zn1–N1	99.91(14)
		O14–Zn2–O11	85.10(15)
		O14–Zn2–N3	79.42(16)
		O14–Zn2–N4	128.00(19)
		O17–Zn2–O11	102.90(16)
		O17–Zn2–O14	120.70(15)
		O17–Zn2–N3	104.76(19)
		O17–Zn2–N4	110.88(19)
		N3–Zn2–O11	152.3(2)
		N4–Zn2–O11	77.31(14)
		N4–Zn2–N3	94.32(13)

Table 3

Hydrogen bonding parameters in **1**

D–H \cdots A	D–H/Å	H \cdots A/Å	D \cdots A/Å	D–H \cdots A/°
Intramolecular interactions				
N(2)–H(2A) \cdots O(5)	0.90	2.39	2.847(6)	112
N(2)–H(2B) \cdots O(4)	0.90	2.44	2.881(6)	110
N(4)–H(4A) \cdots O(13)	0.90	2.35	2.801(6)	111
N(4)–H(4B) \cdots O(12)	0.90	2.38	2.845(6)	112
O(5)–H(5) \cdots N(2)	0.82	2.52	2.847(6)	106
Intermolecular interactions				
O(1)–H(1) \cdots O(9) ⁱ	0.66	1.95	2.572(6)	158
O(2)–H(2) \cdots O(9) ⁱⁱ	0.82	1.91	2.707(5)	164
O(3)–H(3) \cdots O(15)	0.82	2.15	2.900(5)	151
N(1)–H(1B) \cdots O(18)	0.90	2.24	2.980(6)	139
N(2)–H(2A) \cdots O(18)	0.90	2.16	2.945(5)	145
N(2)–H(2B) \cdots O(20) ⁱⁱⁱ	0.90	2.10	2.949(6)	156
N(3)–H(3B) \cdots O(8) ^{iv}	0.90	2.22	3.014(6)	147

Table 3 (continued)

O(4)–H(4)···O(10) ^v	0.82	2.03	2.805(4)	157
O(4)–H(4)···O(13) ^{vi}	0.82	2.46	2.742(5)	101
N(4)–H(4A)···O(10) ^{vii}	0.90	2.13	2.923(6)	146
N(4)–H(4B)···O(8) ^{iv}	0.90	2.19	3.021(6)	153
O(6)–H(6)···O(10) ⁱ	1.05(6)	1.60(6)	2.635(6)	171(5)
O(11)–H(11)···O(20) ⁱⁱⁱ	0.82	1.97	2.629(6)	136
O(12)–H(12)···O(6) ^{iv}	0.82	2.14	2.946(5)	170
O(13)–H(13)···O(4) ^{viii}	0.82	2.26	2.742(5)	118
O(13)–H(13)···O(20) ^{vi}	0.82	2.35	3.082(4)	150
O(14)–H(14)···O(19) ⁱⁱⁱ	0.82	1.96	2.589(6)	133
O(15)–H(15)···O(19) ^{ix}	0.82	1.91	2.718(6)	166
O(16)–H(16)···O(2) ^{iv}	0.82	2.14	2.893(6)	154

ⁱ = x, 1+y, z; ⁱⁱ = -x, 1/2+y, 1-z; ⁱⁱⁱ = x, -1+y, z; ^{iv} = 1+x, y, z; ^v = -x, 1/2+y, -z; ^{vi} = 1-x, -1/2+y, -z; ^{vii} = 1+x, 1+y, z; ^{viii} = 1-x, 1/2+y, -z; ^{ix} = 1-x, -1/2+y, 1-z

EXPERIMENTAL

Materials and methods

All starting materials were of reagent grade quality and were used as received from commercial sources without further purification.

A mixture of ZnO (0.3 g, 1 mmol), H₃tris (0.3 g, 1 mmol), 1,3-benzenedicarboxylic acid (0.17 g, 1 mmol), and Et₃N (0.2 g, 2 mmol) in methanol (20 mL) was sealed in a Teflon-lined stainless steel container and heated at 110 °C for 30 hours, then slowly cooled to room temperature. The resulted colorless crystals were washed with methanol and dried in air. Yield: 60%. IR (KBr, cm⁻¹): 3457m, 3310m, 3249m, 3157w, 2944w, 1623vs, 1602s, 1579vs, 1551s, 1483m, 1436s, 1374vs, 1079s, 1052s, 752m, 718s.

Physical measurements

IR spectrum was recorded on KBr pellets in the 4000–400 cm⁻¹ range using a Bruker TENSOR 27 FTIR Spectrometer. PXRD diffractions pattern was recorded on a Bruker D8 ADVANCE diffractometer. The TG/DTG/DTA+FTIR measurement was performed on a Netzsch STA 409 PC thermal analyzer coupled to a Bruker Tensor 27 FTIR spectrometer equipped with a TG-IR gas cell. The sample was placed in a cylindrical Al₂O₃ holder and heated in synthetic air flow (100 ml min⁻¹, purity 99.999%), from room temperature to 600 °C, at a heating rate of 10 °C min⁻¹. An empty Al₂O₃ holder was used as a reference. The FTIR spectra were collected continuously during measurements in the wavenumber range 4000 – 650 cm⁻¹ at a resolution of 4 cm⁻¹.

Crystal structure determination

X-ray diffraction measurements were performed on an Xcalibur Eos 455 diffractometer operating with Mo K α (λ = 0.71073 Å) X-ray tube with 456 graphite monochromator. The structure was solved by direct methods and refined by full-matrix least squares techniques based on F^2 . The non-H atoms were refined with anisotropic displacement parameters. Calculations were performed using SHELX-97⁸ crystallographic software package. A summary of the crystallographic data and the structure refinement for **1** is given in Table 1. CCDC reference number: 1419948.

Acknowledgements: Financial support from the Roumanian Ministry of Education CNCS-UEFISCDI (Project PN-II-RUTE-2012-3-0390) is gratefully acknowledged.

REFERENCES

- See, for example: (a) C. Janiak, *Dalton Trans.*, **2003**, 2781; (b) B. Moulton and M. J. Zaworotko, *Chem. Rev.*, **2001**, *101*, 1629; (c) S. Kitagawa, R. Kitaura and S.-I. Noro, *Angew. Chem., Int. Ed.*, **2004**, *43*, 2334; (d) J. R. Long and O. M. Yaghi, *Chem. Soc. Rev.*, **2009**, *38*, 1213; (e) D. Maspoch, D. Ruiz-Molina and J. Veciana, *Chem. Soc. Rev.*, **2007**, *36*, 770; (f) G. Ferey, *Chem. Soc. Rev.*, **2008**, *37*, 191; (g) L. J. Murray, M. Dincă and J. R. Long, *Chem. Soc. Rev.*, **2009**, *38*, 1294.
- (a) A. M. Beatty, *Coord. Chem. Rev.*, **2003**, *246*, 131; (b) G. R. Desiraju, in: F. Vögtle, J. F. Stoddart, M. Shibasaki (Eds.), "Stimulating Concepts in Chemistry", Wiley VCH, Weinheim, 2000, p. 293; (c) C. B. Aakeröy and K. R. Seddon, *Chem. Soc. Rev.*, **1993**, *22*, 397; (d) J. C. MacDonald and G. M. Whitesides, *Chem. Rev.*, **1994**, *94*, 2383; (e) L. Yang, X. Tan, Z. Wang and X. Zhang, *Chem. Rev.*, **2015**, *115*, 7196.
- (a) T. R. Cook, Y.-R. Zheng and P. J. Stang, *Chem. Rev.*, **2013**, *113*, 734; (b) E. Tynan, P. Jensen, P. E. Kruger, A. C. Leesa and M. Nieuwenhuyzen, *Dalton Trans.*, **2003**, 1223; (c) M. Lackinger and W. Heckl, *Langmuir*, **2009**, *25*, 11307.
- (a) X. M. Zhang, *Coord. Chem. Rev.*, **2005**, *249*, 1201; (b) X.-M. Chen and M.-L., Tong, *Acc. Chem. Res.*, **2007**, *40*, 162; (c) Y. Zhao, K. Li and J. Li, *Z. Naturforsch.*, **2010**, *65b*, 976.
- C. Paraschiv, A. Cucos, S. Shova, A. M. Madalan, C. Maxim, D. Visinescu, B. Cojocaru, V. I. Parvulescu and M. Andruh, *Crystal Growth Des.*, **2015**, *15*, 799.
- (a) B. K. Babu, A. R. Biju, S. Sunkari, M. V. Rajasekharan and J. -P. Tuchagues, *Eur. J. Inorg. Chem.*, **2013**, 1444; (b) A. Company, L. Gómez, J. M. López Valbuena, R. Mas-Ballesteé, J. Benet-Buchholz, A. Llobet and M. Costas, *Inorg. Chem.*, **2006**, *45*, 2501.
- A. W. Addison, T. N. Rao, J. Reedijk, J. van Rijn and G. C. Verschoor, *J. Chem. Soc., Dalton Trans.*, **1984**, 1349.
- G. M. Sheldrick, *Acta Crystallogr.*, **2008**, *A64*, 112.